

# AN INVESTIGATION OF THE EFFECT OF MACHINING PARAMETERS ON STRAIN-INDUCED MARTENSITE FORMATION DURING TURNING IN AN AUSTENITIC STAINLESS STEEL

## Izabel Fernanda Machado

Department of Mechatronics and Mechanical Systems Engineering- Polytechnic School – USP  
Av. Prof. Mello Moraes, 2231 05508-900 São Paulo S. P. Brazil.  
E-mail: machadoi@usp.br

## João Paulo Pereira Marcicano

Department of Mechatronics and Mechanical Systems Engineering- Polytechnic School – USP  
Av. Prof. Mello Moraes, 2231 05508-900 São Paulo S. P. Brazil.  
E-mail: marcican@usp.br

## Larissa Driemeier

Department of Mechatronics and Mechanical Systems Engineering- Polytechnic School – USP  
Av. Prof. Mello Moraes, 2231 05508-900 São Paulo S. P. Brazil.  
E-mail: driemeie@usp.br

## Carlos Alberto Nunes Dias

Department of Mechatronics and Mechanical Systems Engineering- Polytechnic School – USP  
Av. Prof. Mello Moraes, 2231 05508-900 São Paulo S. P. Brazil.  
E-mail: candias@usp.br

**Abstract.** Phase transformations occur in austenitic stainless steels during heat treatments and also during intense plastic deformation. Strain-induced martensite is a kind of phase transformation that can occur during machining of austenitic stainless steels due to intense plastic deformation in the chip formation region. Strain-induced martensite causes a microstructural transformation, volume variation, increase in surface hardness as well as an increase of cutting forces during the machining. The aim of this work is to study strain-induced martensite formation in the AISI 304 austenitic stainless steel during turning. The strain-induced martensite formation was investigated by using magnetic measurements and microhardness. The cutting force and the surface roughness were also evaluated.

**Keywords.** austenitic stainless steel, turning, strain, work hardening, martensite

## 1. Introduction

The objective of machining is to obtain a component with the required dimensional accuracy and surface finish. Most of the machining processes involve high plastic strain, which occurs in the chip formation region. The cutting process, during turning, involves three regions by using the orthogonal cutting model (Shaw, 1986). The first area is alongside the shear plane, the second is the region between the chip and the tool and the last is the surface turned. This study is concerned with the first and the third regions, which are strongly influenced by plastic strain. These high strains cause microstructural modifications on the surface. Surface finish is a measure of the quality of a machined surface because it can affect the component performance, such as for instance in fatigue or creep. It is related to surface roughness, hardness, microstructural changes and as a consequence in residual stresses (Shaw, 1986; Grzesik, 1996 and Jang et al.; 1996). In order to improve the fabrication quality it is necessary to study the surface quality of machined metals and alloys. Models relating to cutting force, among other machining parameters have been proposed in literature [Grzesik, 1996; Jang et al.; 1996; Kovak et al., 1997; Abouelatts et al., 2001; Lin et al., 2001 and Saï et al., 2001]. Besides that almost all cutting energy is consumed for chip formation. The more easily the chips are formed the cheaper the machining of the component is. In conclusion, the machinability of a material plays an important role in component dimensions and its mechanical properties as well as economical factors.

Despite their poorer machinability as compared to other classes of steels, austenitic stainless steels have been widely utilized because of their combination of mechanical properties and high corrosion resistance, (Lacombe et al., 1993; Jang et al.; 1996 and M'Saoubi et al., 1999). The problems related to difficulties of machining of austenitic stainless steels are: tool wear, poor surface finish, long and stringy chips and low cutting speed (Fang et al., 1996, Jang et al.; 1996 and M'Saoubi et al., 1999). These difficulties are mainly caused by their high work hardening rate, low thermal conductivity and the tendency to strain-induced martensite formation (Tessler et al., 1992; Lacombe et al., 1993 and M'Saoubi et al., 1999). During turning, plastic deformation of austenitic stainless steels causes high mechanical and microstructural sensitivity in surface, increasing the cutting force among other points, and the surface finish, which can affect later utilization of the produced part. The machinability of some austenitic stainless steel can be improved by sulphur addition. The sulphur addition propitiates the formation of manganese sulfide inclusions that make chip breaking easier. The sulphur also works as a lubricant. However, the sulphur addition causes the loss in mechanical properties and corrosion resistance among other effects.

Phase transformations can occur in austenitic stainless steels during heat treatments and also during intense plastic strain (Lacombe et al., 1993 and Padilha et al., 1994). Austenitic stainless steels are not susceptible to martensite

formation during cooling. On the other hand, martensite can be formed during cold work. It is named strain-induced martensite, as cited above (Lacombe et al., 1993 and Padilha et al., 1994). There are two types of strain-induced martensite the  $\alpha'$  and the  $\epsilon$  martensite. The quantities of each type of martensite depend on the level of deformation. The  $\alpha'$  martensite formation replaces the  $\epsilon$  martensite with an increase of deformation level and only  $\alpha'$  martensite is expected for high levels of deformation. The  $\alpha'$  martensite can be measured by using a ferritoscope, because it is a ferromagnetic phase or by X ray diffraction technique. This phase transformation has been studied (Hecker et al., 1982; Murr et al., 1982; Huang et al. 1989; Krauss, 1989) because of its importance in mechanical processes such as forming. As a consequence of the workhardening and the strain-induced martensite formation during machining. An increase of the surface hardness in austenitic stainless steels affects directly tool wear and surface finish. The strain-induced martensite formation is strongly influenced by the composition of the austenitic stainless steel. The following relations (Krauss, 1989) show the influence of composition on strain-induced martensite formation. At a given strain, martensite formation decreases with an increase in temperature (Huang et al., 1989; Krauss et al., 1989).

$$Md_{50/30}(^{\circ}C) = 413 - 9.5Ni - 13.7Cr - 8.1Mn - 9.2Si - 18.5Mo - 462(C+N) \quad (1)$$

(Md 50/30( $^{\circ}C$ ) is the temperature at which 50% martensite is formed by 30% true strain in tension)

$$Md_{10/45}(^{\circ}C) = 433 - 27.6Ni - 7.7Cr - 16.2Mn - 27.2Si - 11.3Mo - 170(C+N) \quad (2)$$

(Md 10/45( $^{\circ}C$ ) is the temperature at which 10% martensite is formed by 45% true strain in tension)

The strain-induced martensite formation is also influenced by plastic strain and strain rate. The higher the strain rate, at a given temperature, the higher the volumetric fraction of strain-induced martensite, although at lower temperatures the effect of strain rate is stronger (Huang et al., 1989). Another work (Hecker et al. 1982; Murr et al., 1982) showed that the increase in the strain rate at strains greater than 0.25 can cause a suppression of strain-induced martensite because of the occurrence of adiabatic heating. This work (Hecker et al. 1982; Murr et al., 1982) also showed that strain-induced martensite is more effectively induced during biaxial tension than in axial tension. More complex states of strain seem to propitiate martensite formation.

The sulphur addition is not the best solution for poor machinability of austenitic stainless steels as cited above. The study of machinability of austenitic stainless steels is an important topic from the industrial and academic point of view. The main objective of this study is to relate machining parameters, such as feed, to workhardening and strain-induced martensite in austenitic stainless steel. In this work the AISI 304 austenitic stainless steel was turned with different feeds and cutting depths. Roughness, microhardness and magnetic measurements were done on the turned surface to evaluate the properties. Cutting force was also measured in some tests. Chip shear strain was calculated and related with literature results.

## 2. Materials and Methods

The material utilized in this study was a rolling bar with 25.4 mm diameter of AISI 304 austenitic stainless steel. The nominal composition of the steel studied is showed in table 1. The samples used in the tests were 70 mm long and had a 25.4 mm diameter.

Table 1 – Nominal composition (wt%) of AISI 304 austenitic stainless steel.

Steel	%Cr	%Ni	%C (max)	%Mn (max)	%Si (max)	%Mo	%S (max)
AISI 304	18.00-20.00	8.00-10.00	0.08	2.00	1.00	-	0.03

The material was turned by using a universal lathe equipped with a load cell. The samples were fixed in three-jaw chucks, the tailstock was not utilized. The tool utilized was CNMG120512 type, TiN coated. The toolholder was a PCLNR2525M12 type. The side cutting edge angle utilized was 0 $^{\circ}$ , the rake angle used was +4 $^{\circ}$  and relief angle was 8 $^{\circ}$ . The cutting speed of the tests was 88 mm/min and no cutting fluid was used.

The samples were turned in different conditions. Feeds utilized in the tests are shown in table 2. Two different feed (f) - cutting depth (d) relations were used in this study. In the first set of tests the relation used was f/d=1 and in the second set of tests the relation used was f/d=0.2 as shown in table 2.

During turning, cutting force was also evaluated in the set of tests done on f/d=1 relation. The cutting force was measured by using a load cell connected to an acquisition board with a power source, an amplifier and a low pass filter. The load cell was calibrated by applying force in a spindle linked to a mechanical dynamometer. A 152N/V calibration constant was obtained. During the turning test, the sample rate utilized was 2000 samples/second. The results were acquired during a 10-second test. The cutting force obtained was based on an average result of 8000 samples. These points were chosen from the 20000 samples.

Table 2 – Feeds utilized in machining tests of AISI 304 austenitic stainless steel. f (mm/rev) is the feed and d (mm) is the cutting depth.

Test	1	2	3	4	5	6	7	8	9
	f(mm/rev)	f(mm/rev)	f(mm/rev)	f(mm/rev)	f(mm/rev)	f(mm/rev)	f(mm/rev)	f(mm/rev)	f(mm/rev)
f/d=1	0.060	0.067	0.082	0.104	0.149	0.205	0.327	0.428	0.595
f/d=0.2	0.060	0.067	0.082	0.104	0.149	0.205	0.327	-	-

The mean roughness (Ra) of the turned surfaces was measured by using a surface profilometer Taylor Hobson model surtronic 3+. The cutoff ( $\lambda_c$ ) utilized was the one recommended in ISO4288 Standard (0.8 mm or 2.5 mm selected based on mean roughness). The roughness was measured only once in each turned sample. The confidence interval was calculated based on t Student distribution with 95% confidence level, using the number of elements and sample standard deviation.

The Vickers microhardness was measured by using a 10 g load (HV 0.01). The measures were done in the turned surface of all the specimens. About 6 measures were done in each sample.

The presence of magnetic phases was detected by using a permanent magnet. In some cases it was possible to measure the amount of ferromagnetic phases by using the magnetic induction method (Fisher Permascope®, with a 0.1% ferrite detection limit). The measure of the amount of magnetic phases, mainly in the chips, was limited by the size of the sample.

Scanning electron microscopy was also used to observe the morphology of chips formed. Two samples were selected to be observed.

### 3. Results and Discussion

In this work the influence of machining parameters on plastic strain and roughness was studied by analyzing the coefficient of correlation between surface microhardness and chip shear strain and also by analyzing the coefficient of correlation between mean roughness (Ra) and chip shear strain. The results and discussion will be presented in different sections as follows: chip shear strain versus microhardness, roughness versus feed, cutting force versus feed and characterization of chips morphology.

#### 3.1 Chip Shear Strain versus Microhardness

Table 3 shows the results of deformed chip thickness ( $t'$ ) with confidence interval (CI95%) as a function of feed (f) for the set of tests done on f/d=1. Table 4 shows the results of deformed chip thickness ( $t'$ ) with a confidence interval (CI95%) as a function of feed (f) for the set of tests done on f/d=0.2.

The chip shear strain ( $\epsilon_o$ ) is given by equation (3) (Ferraresi, 1977).

$$\epsilon_o = \frac{1 + R_c^2 - 2R_c \sin \gamma}{R_c \cos \gamma} \quad (3)$$

Where  $R_c$  is the cutting ratio,  $\gamma$  is the rake angle. The cutting ratio ( $R_c$ ) is calculated by division of undeformed chip thickness (t) by deformed chip thickness ( $t'$ ). The undeformed chip thickness has the same value of feed (f). Table 5 shows the chip shear strain ( $\epsilon_o$ ) calculated for the all the test.

Table 5 shows the results of chip shear strain ( $\epsilon_o$ ) calculated for the all the test by using equation (3).

Table 3 – Results of deformed chip thickness ( $t'$ ) with confidence interval (CI95%) as a function of feed (f) for the set of tests done on f/d=1. Cutting depth is given by d (mm).

f (mm/rev)	$t'$ (mm)	CI95% $t'$ (mm)
0.060	0.07	0.01
0.067	0.09	0.01
0.082	0.10	0.01
0.104	0.12	0.01
0.149	0.17	0.01
0.205	0.22	0.02
0.327	0.36	0.03
0.428	0.48	0.02
0.595	0.66	0.03

Table 4 – Results of deformed chip thickness ( $t'$ ) with a confidence interval (CI95%) as a function of feed ( $f$ ) for the set of tests done on  $f/d=0.2$ . Cutting depth is given by  $d$  (mm).

$f$ (mm/rev)	$t'$ (mm)	CI95% $t'$ (mm)
0.060	0.10	0.02
0.067	0.17	0.01
0.082	0.14	0.02
0.104	0.20	0.01
0.149	0.22	0.03
0.205	0.37	0.03
0.327	0.47	0.12

Table 5 - The chip shear strain ( $\epsilon_o$ ) calculated for the all the tests.  $f$  (mm/revolution) is the feed and  $d$  (mm) is the cutting depth.

$f$ (mm/rev)	$\epsilon_o$ ( $f/d=1$ )	$\epsilon_o$ ( $f/d=0.2$ )
0.060	1.89	2.09
0.067	1.96	2.82
0.082	1.89	2.13
0.104	1.88	2.34
0.149	1.89	2.00
0.205	1.87	2.22
0.327	1.87	2.00
0.428	1.88	-
0.595	1.88	-

The results of chip shear strain and shear angles were reliable to the flow localization analysis for the case of orthogonal cutting existing in the literature (Semiatin, 1984). The results of Vickers microhardness measurements on the machined surface are shown in tables 6 and 7.

Tables 6 and 7 show an increase of microhardness on the machined surface with a decrease of feed. The increase of microhardness can be explained by the strong workhardening and strain-induced martensite formation. The strong workhardening is a well-known behavior of this material because of, among other factors, its low stacking fault. The strain-induced martensite is a phase transformation that also increases mechanical properties such as hardness and yield strength. The tendency for this phase transformation to occur can be estimated by using equations (1) and (2). On calculating  $M_d$  for AISI 304 austenitic stainless steels one can find values around the room temperature. Besides, the work realized by Hecker et al. (Hecker et al., 1982) showed that when high strain rates are used an amount of about 50% martensite is formed in AISI 304 steel that is an expressive quantity. The increase in microhardness can be an indirect measure of strain-induced martensite formation. However, the strain-induced martensite, which is a ferromagnetic phase, was not identified by using a ferriscope on machined surface. The formation of this phase probably occurred but the layer affected was very small and the strain was not uniform, so the measures could be out of the detection limit of the equipment. Besides that the bar of the AISI 304 austenitic steel had a slight magnetism of about 0.3% due to  $\delta$ -ferrite. After turning, the measures of magnetism acquired were also around 0.3%. This kind of measure does not seem to be appropriate to identify strain-induced martensite in this work. Magnetic measures were also done in chips formed during turning. In this case magnetism was also detected, but it was not possible to quantify the amount of martensite because of the limitations of the equipment. However the use of a permanent magnet made it possible to identify levels of magnetism in the chips of about 2%. X-ray measurements will be necessary to quantify the amounts of martensite formed.

Table 6 and 7 also show that the highest values of microhardness were obtained for the set of tests done on  $f/d=1$ . These results can be explained by the different strain states in the case of set of tests done on  $f/d=1$  and  $f/d=0.2$ . In the second case, the state of strain is near a plane one whereas the first case is not. In the case of  $f/d=1$ , i.e., the lowest cutting depth, the material at the trailing edge of the tool is subjected to a high normal stress, causing a material flow to the side to alleviate this stress. In this case, the undeformed chip thickness is probably zero or near zero (Shaw, 1986). The material flow to the side and high strain in the chip can affect the amount of the local strain in the surface. The coefficients of correlation microhardness and chip shear strain obtained are also an indication of influence of cutting depth on the strain state during the cutting of material. In the case of  $f/d=1$  was found a good correlation which does not seem to exist in the other case ( $f/d=0.2$ ).

Table 6 – Results of microhardness (HV 0.01) of the machined surface as a function of feed for the set of tests done on  $f/d=1$ .  $f$  (mm/revolution) is the feed and  $d$  (mm) is the cutting depth.

$f$ (mm/rev)	Microhardness (HV 0.01)	CI95% Microhardness (HV 0.01)
0.060	549	75
0.067	636	60
0.082	447	60
0.104	367	37
0.149	334	50
0.205	319	34
0.327	326	25
0.428	307	38
0.595	298	47

Table 7 – Results of microhardness (HV 0.01) of the machined surface as a function of feed for the set of tests done on  $f/d=0.2$ .  $f$  (mm/revolution) is the feed and  $d$  (mm) is the cutting depth.

$f$ (mm/rev)	Microhardness (HV 0.01)	CI95% Microhardness (HV 0.01)
0.060	392	31
0.067	310	76
0.082	276	25
0.104	315	49
0.149	343	33
0.205	257	68
0.327	272	45

Figure 1 shows the results of Vickers microhardness (HV 0.01) versus chip shear strain ( $\epsilon_0$ ).

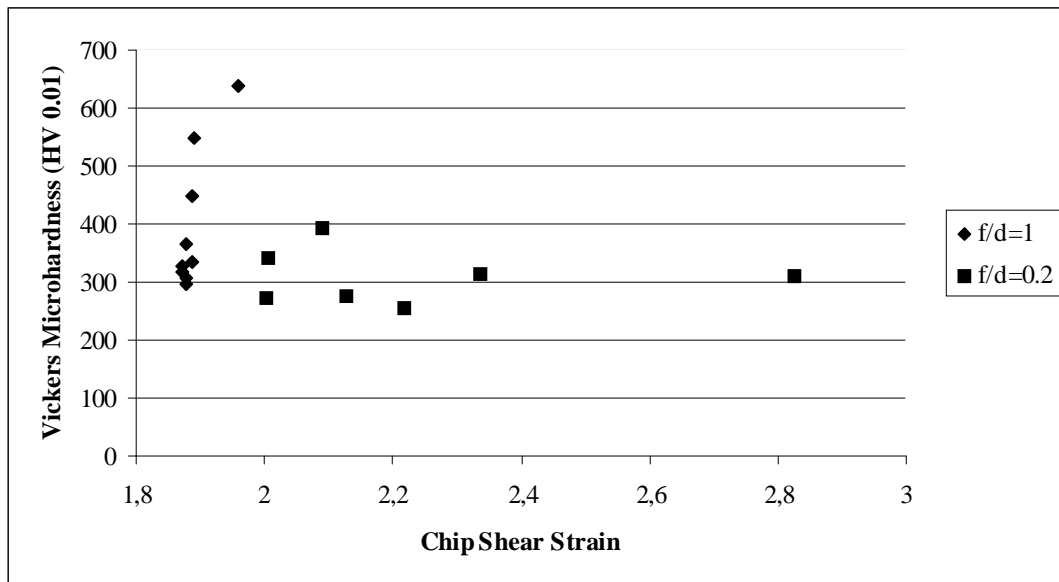


Figure 1. Results of Vickers microhardness (HV) versus chip shear strain ( $\epsilon_0$ ).

The results of figure 1 shows existing dependence between surface microhardness and chip shear strain for the ratio cutting depth and feed of 1 ( $f/d=1$ ). On the other hand for the ratio cutting depth and feed of 5 ( $f/d=0.2$ ) no dependence was observed. This behavior can be verified by correlation coefficient analysis. It was obtained for  $f/d=1$  a correlation coefficient of 0.83 and for  $f/d=0.2$  a correlation coefficient of  $-0.07$  which means a poor dependence of microhardness and chip shear strain for the second case ( $f/d=0.2$ ).

### 3.2 Roughness versus Feed

The roughness of the surface can be determined by geometrical aspects, which depend on the feed and tool nose radius. Roughness is also influenced by tool wear, vibrations and plastic strain that occurs due to chip formation.

Table 8 shows the results of mean roughness (Ra) as a function of feed (f) for the set of tests done on  $f/d=1$ . Table 9 shows the results of mean roughness (Ra) as a function of feed (f) for the set of tests done on  $f/d=0.2$ . Figure 2 shows the mean roughness (Ra) versus feed (f).

Table 8 – Results of mean roughness (Ra) as a function of feed (f) for the set of tests done on  $f/d=1$ . d (mm) is the cutting depth.

f (mm/rev)	Ra ( $\mu\text{m}$ )
0.060	1.24
0.067	0.82
0.082	0.76
0.104	1.02
0.149	2.08
0.205	1.66
0.327	2.52
0.428	5.06
0.595	8.26

Table 9 – Results of mean roughness (Ra) as a function of feed (f) for the set of tests done on  $f/d=0.2$ . d (mm) is the cutting depth.

f (mm/rev)	Ra ( $\mu\text{m}$ )
0.060	0.74
0.067	0.60
0.082	0.58
0.104	0.54
0.149	0.80
0.205	1.26
0.327	1.48

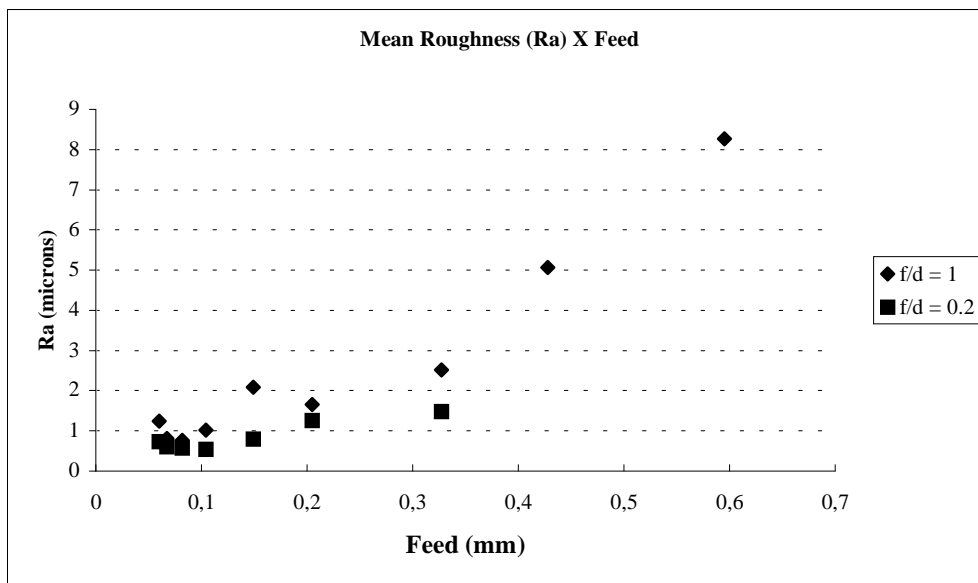


Figure 2. Results of the mean roughness (Ra) versus feed (f) for the set of tests done on  $f/d=1$  and for the set of tests done on  $f/d=0.2$ . d (mm) is the cutting depth.

The results in figure 2 show that the roughness is not strongly influenced by feed at low feeds. In the tests realized using low feeds the roughness could be determined by other factors, such as surface deformation due to the chip formation as discussed in item 3.1. When low feeds are used, the material at the trailing edge of the tool is subjected to a high normal stress, causing a material flow to the side to alleviate this stress. In this case, the undeformed chip thickness gradually goes to zero (Shaw, 1986). The material flow to the side and high strain in the chip can affect the amount of the local strain in the surface and also the roughness.

The results show that there is a slight dependence between mean roughness ( $R_a$ ) and chip shear strain in the tests using the following feeds: 0.06, 0.067, 0.082, 0.014 mm/rev. For  $f/d=1$  the correlation coefficient obtained for the four lowest feeds was -0.45 and for  $f/d=0.2$  the correlation coefficient was -0.35. It was also observed that there was a geometrical contribution on roughness. Therefore the correlation coefficient was calculated between mean roughness ( $R_a$ ) logarithm and feed ( $f$ ) logarithm, because the depth of tool marks is proportional to square of feed. For  $f/d=1$  the correlation coefficient of logarithm was -0.24 and for  $f/d=0.2$  the correlation coefficient of logarithm was -0.87. These results show for the set of tests done on  $f/d=0.2$  the roughness can be mainly caused by geometrical contribution. On the other hand, for the set of tests done on  $f/d=1$  the roughness can be mainly caused by the strain in the turned surface.

### 3.3 Cutting Force versus Feed

Table 10 shows the results of cutting force ( $F_c$ ) as a function of feed ( $f$ ) for the set of tests done on  $f/d=1$ . The results of cutting force showed an expected relation with feed.

Table 10 – Results of cutting force ( $F_c$ ) as a function of feed ( $f$ ) for the set of tests done on  $f/d=1$ .  $d$  (mm) is the cutting depth.

$f$ (mm/rev)	$F_c$ (N)
0.060	38
0.067	58
0.082	55
0.104	83
0.149	133
0.205	188
0.327	318
0.428	537
0.595	*

\*The cutting force was not evaluated in the last test ( $f=0.595$  mm/rev) because the full-scale was reached.

Figure 3 shows the results of  $k_s$  (specific pressure of cutting) versus feed ( $f$ ).

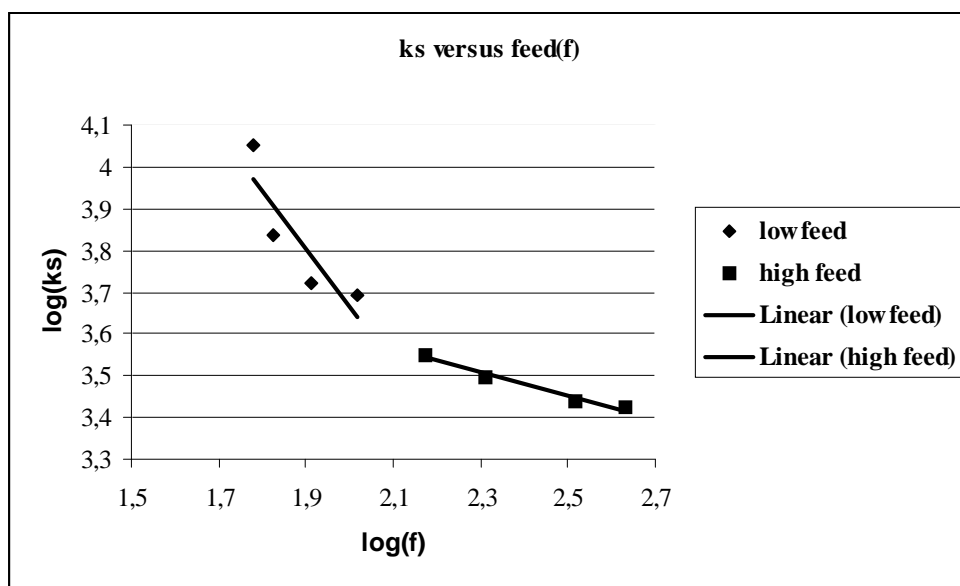


Figure 3. Log ( $k_s$ ) ( $k_s$ ,  $N/mm^2$ ) versus log ( $f$ ) (mm/rev),  $k_s$  means specific pressure of cutting and  $f$  indicates feed.

According to Kienzle model  $k_s$  is given by equation (4):

$$k_s = \frac{k_{s1}}{(f \sin \chi)^z} \quad (4)$$

$k_{s1}$  and  $z$  are coefficients used in Kienzle model (Ferraresi, 1977). A change in  $k_{s1}$  and  $z$  for feeds higher than 0.1 mm/rev can be observed. This behavior can be explained by the change of mechanism of chip formation.

### 3.4 Characterization of Chips Morphology

The following figures show the results of observations of chips, obtained using feed 0.060 mm/rev and 0.585 mm/rev in the set of tests done on  $f/d=1$ , by using scanning electron microscopy with secondary electrons. The chips were chosen as representative samples for low and high feed, respectively. In the majority of tests the chips were continuous. The chips obtained using the lowest feed showed a more inhomogeneous shear than when the highest one was used. The occurrence of high inhomogeneous shear of chips seems to be related to the highest surface microhardness. Lower feeds also produced chips with undeformed chip thickness lower than when higher feeds were utilized. The amount of strain-induced martensite probably was concentrated in shear-localized region. Perhaps lower feeds can cause more uniform strain-induced martensite formation.

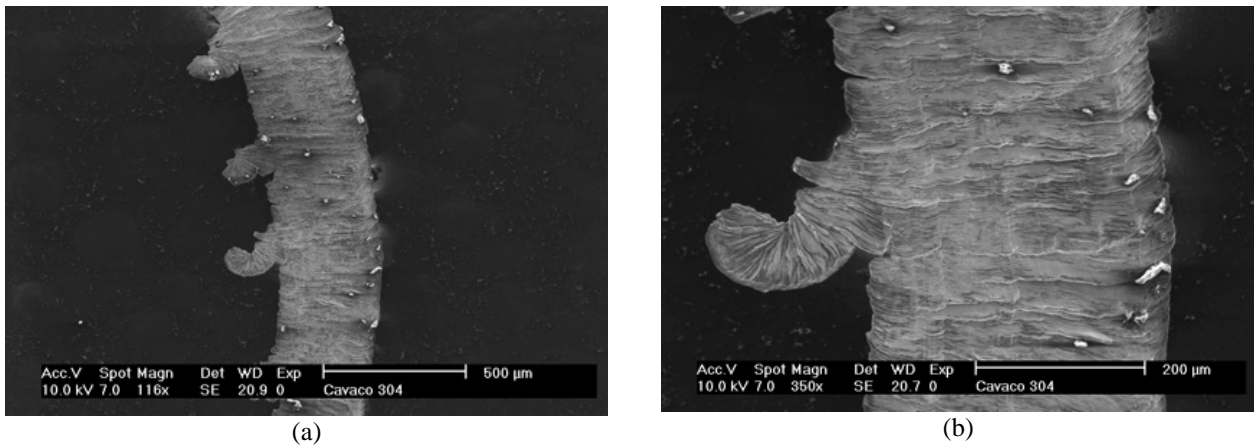


Figure 4. Chip morphology obtained in the turning test using feed of 0.060 mm/rev in the set of tests done on  $f/d=1$ . Shear-localized can be observed. Scanning electron microscopy with secondary electrons. (a) and (b) indicate the different magnitudes utilized.

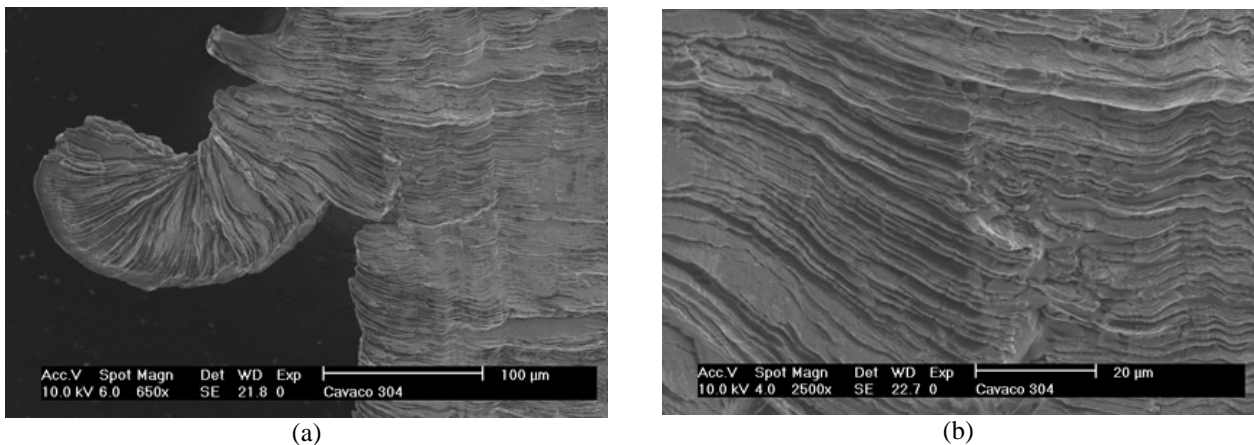


Figure 5. Chip morphology obtained in the turning test using feed of 0.060 mm/rev in the set of tests done on  $f/d=1$ . Shear-localized can be observed. Scanning electron microscopy with secondary electrons. (a) and (b) indicate the different magnitudes utilized.



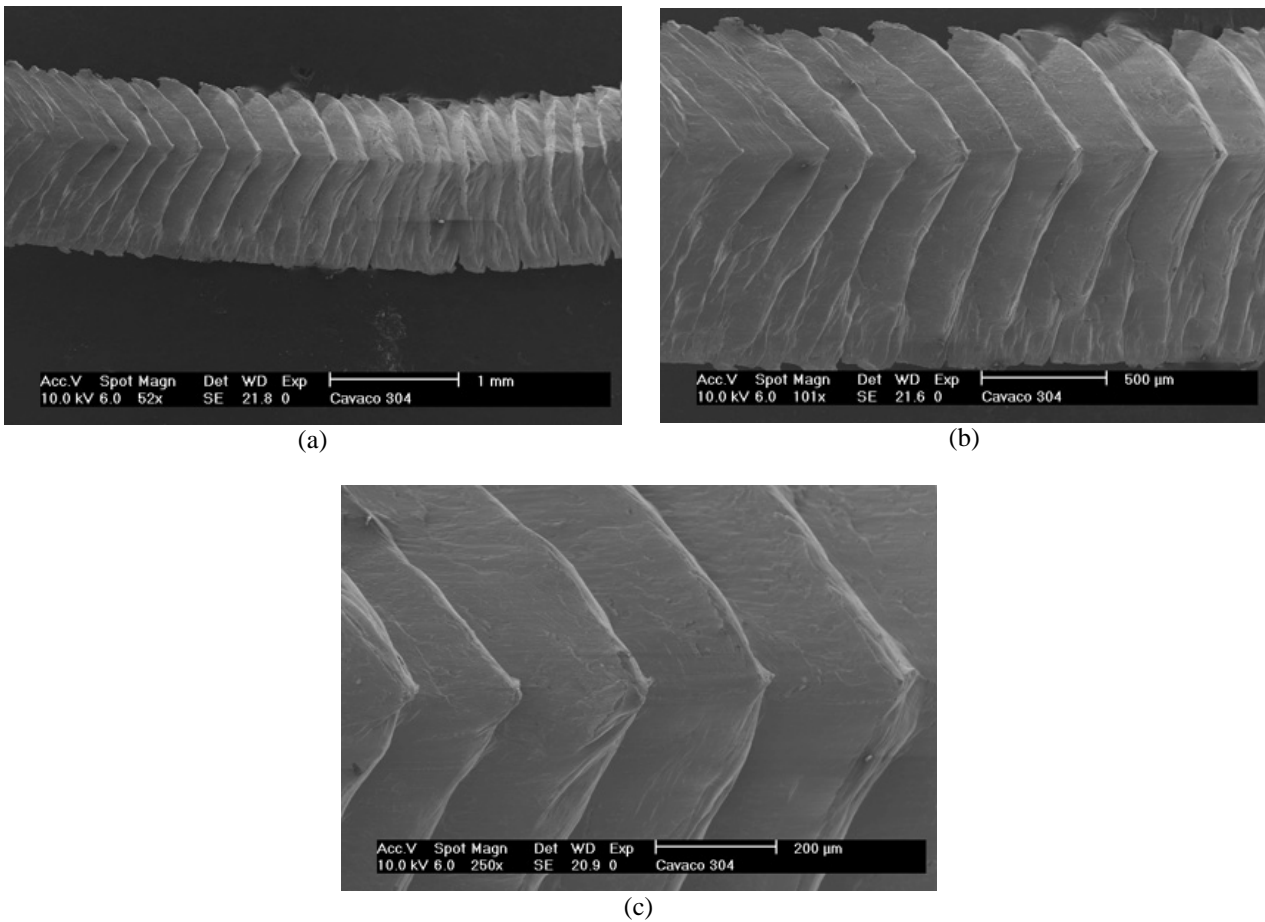


Figure 6. Segmented chip morphology obtained in the turning test using feed of 0.585 mm/rev in the set of tests done on  $f/d=1$ . Shear-localized can be observed. Scanning electron microscopy with secondary electrons. (a), (b) and (c) indicate the different magnitudes utilized.

#### 4. Conclusions

The following conclusions are based on the results presented in this study:

1. Strain-induced martensite was identified mainly in the chips through the use of magnetic measurements. In the turned surface it was not identified through the use of magnetic measurements probably because of the detection limit of the equipment. The microhardness measurements are an indication of workhardening and strain-induced martensite formation although it is not conclusive.
2. A different behavior was observed in workhardening, evaluated by microhardness measurements, and roughness in the set of tests done on  $f/d=1$  and  $f/d=0.2$ . This behavior can be caused by different state of strain during the chip formation. In the set of tests done on  $f/d=0.2$  a plane strain state was expected unlike in the set of tests done on  $f/d=1$ .

#### 5. Acknowledgments

The authors are grateful to LFS (Laboratório de Fenômenos de Superfície, Mechanical Department of Polytechnic School of University of São Paulo) for Vickers microhardness measurements and Dr. Márcilio Alves for equipment that made possible to evaluate cutting force. The authors are also grateful to Dr. Eng. Márcio Ferreira Hupalo for scanning electron microscopy (Metallurgical and Materials Department of Polytechnic School of University of São Paulo).

#### 6. References

- Abouelatta, O. B.; Máld, J., 2001, "Surface roughness prediction based on cutting parameters and tool vibrations in turning operations", *Journal of Materials Processing Technology*. Vol. 118, pp. 269-277.
- Fang, X. D.; Zhang, D., 1996, "An investigation of adhering layer formation during tool wear progression in turning of free-cutting stainless steels", *Wear*, Vol. 197, pp. 169-178.
- Ferraresi, D., 1977, "Fundamentos da Usinagem dos Metais", Edgard Blücher Ltda, São Paulo.
- Padilha, A. F.; Guedes, L. C., 1994, "Aços inoxidáveis austeníticos microestrutura e propriedades", Hemus, São Paulo.
- Grzesik, W. A., 1996, "Revised model for predicting surface roughness in turning", *Wear*. Vol. 194. pp. 143-148.

- Hecker, S. S.; Stout, M.G.; Staudhammer, K.P. and Smith, J.L., 1982, 'Effects of strain state and strain rate on deformation-induced transformation in 304 stainless steel: Part I. Magnetic measurements and mechanical behavior', *Metallurgical Transactions*, Vol. 13, pp.619-626.
- Huang, G.L.; Matlock, D.K. and Krauss, G., 1989, 'Martensite formation, strain rate sensitivity, and deformation behavior of type 304 stainless steel sheet', *Metallurgical Transactions*, Vol. 20, pp.1239-1246.
- Jang, D. Y.; Choi, Y.Gu; Kim, H-Gil; Hsio, 1996, 'A. Study of the correlation between surface roughness and cutting vibrations to develop on line roughness measuring technique in hard turning', *International Journal of Machine Tools & Manufacturing*, Vol. 36, pp. 453-464.
- Kovac, P., Sidjanin, L., 1997, 'Investigation of chip formation during milling'. *International Journal of Production Economics*, Vol. 51, pp. 149-153.
- Lacombe, P.; Baroux, B.; Beranger, G., 1993, 'Stainless Steels', Les Editions de Physique Les Ulis, France.
- Lin, W. S.; Lee, B. Y.; Wu, C. L., 2001, 'Modeling the surface roughness and cutting force for turning', *Journal of Materials Processing Technology*, Vol. 108, pp. 286-293.
- Meyers, M.; Chawla, 2000, 'Mechanical behavior of materials', Prentice Hall, EUA.
- M'Saoubi, R.; Outeiro, J. C.; Changeoux, B.; Lebrun, J. L.; Mourao Dias, A., 1990, 'Residual stress analysis in orthogonal machining of standard and resulfurized AISI 316L steel', *Journal of Materials Processing Technology*, Vol. 96, pp. 225-233.
- Murr, L.E.; Staudhammer, K.P. and Hecker, S. S., 1982, 'Effects of strain state and strain rate on deformation-induced transformation in 304 stainless steel: Part I. Microstructural study', *Metallurgical Transactions*, Vol. 13, pp.627-635.
- Saï, W. B.; Salh, N. B.; Lebrun, J. L., 2001, 'Influence of machining by finishing milling on surface characteristics', *International Journal of Machine Tools & Manufacturing*, Vol. 41, pp. 443-450.
- Semiatin, S.L.; Jonas, J.J., 1984, 'Formability & Workability of Metals', ASM International, EUA.
- Krauss, G., 1989, 'Steels: heat treatment and processing principles', ASM International, EUA.
- Shaw, M. C., 1984, 'Metal Cutting Principles', Clarendon Press, Great Britain.
- Tessler, M. B.; Barbosa, C. A., 1992, 'A usinabilidade dos aços inoxidáveis'. In: INOX96 (Seminário Brasileiro do Aço Inoxidável), 3., São Paulo, São Paulo, Núcleo Inox, pp. 151-167.